JACC: CARDIOVASCULAR IMAGING
VOL. 12, NO. 8, 2019

PUBLISHED BY ELSEVIER

ORIGINAL RESEARCH

T1 Mapping by Cardiac Magnetic Resonance and Multidimensional Speckle-Tracking Strain by Echocardiography for the Detection of Acute Cellular Rejection in Cardiac Allograft Recipients

Leyla Elif Sade, MD,[a] Tuncay Hazirolan, MD,[b] Hatice Kozan, MD,[a] Handan Ozdemir, MD,[c] Mutlu Hayran, MD, PhD,[d] Serpil Eroglu, MD,[a] Bahar Pirat, MD,[a] Atilla Sezgin, MD,[e] Haldun Muderrisoglu, MD[a]

ABSTRACT

OBJECTIVES The aim of this study was to test the hypothesis that echocardiographic strain imaging, by tracking subtle alterations in myocardial function, and cardiac magnetic resonance T1 mapping, by quantifying tissue properties, are useful and complement each other to detect acute cellular rejection in heart transplant recipients.

BACKGROUND Noninvasive alternatives to endomyocardial biopsy are highly desirable to monitor acute cellular rejection.

METHODS Surveillance endomyocardial biopsies, catheterizations, and echocardiograms performed serially according to institutional protocol since transplantation were retrospectively reviewed. Sixteen-segment global longitudinal strain (GLS) and circumferential strain were measured before, during, and after the first rejection and at 2 time points for patients without rejection using Velocity Vector Imaging for the first part of the study. The second part, with cardiac magnetic resonance added to the protocol, served to validate previously derived strain cutoffs, examine the progression of strain over time, and to determine the accuracy of strain and T1 measurements to define acute cellular rejection. All tests were performed within 48 h.

RESULTS Median time to first rejection (16 grade 1 rejection, 15 grade ≥2 rejection) was 3 months (interquartile range: 3 to 36 months) in 49 patients. GLS and global circumferential strain worsened significantly during grade 1 rejection and ≥2 rejection and were independent predictors of any rejection. In the second part of the study, T1 time ≥1,090 ms, extracellular volume ≥32%, GLS >−14%, and global circumferential strain ≥−24% had 100% sensitivity and 100% negative predictive value to define grade ≥2 rejection with 70%, 63%, 55%, and 35% positive predictive values, respectively. The combination of GLS >−16% and T1 time ≥1,060 ms defined grade 1 rejection with 91% sensitivity and 92% negative predictive value. After successful treatment, T1 times decreased significantly.

CONCLUSIONS T1 mapping and echocardiographic GLS can serve to guide endomyocardial biopsy selectively. (J Am Coll Cardiol Img 2019;12:1601–14) © 2019 by the American College of Cardiology Foundation.

From the [a]Cardiology Department, University of Baskent, Ankara, Turkey; [b]Radiology Department, University of Hacettepe, Ankara, Turkey; [c]Pathology Department, University of Baskent, Ankara, Turkey; [d]Preventive Oncology and Epidemiology Department, University of Hacettepe Cancer Institute, Ankara, Turkey; and the [e]Cardiothoracic Surgery Department, University of Baskent, Ankara, Turkey. All financial support related to this study was provided by the University of Baskent. The authors have reported that they have no relationships relevant to the contents of this paper to disclose.

Manuscript received January 22, 2018; revised manuscript received February 27, 2018, accepted February 28, 2018.

ISSN 1936-878X/$36.00 https://doi.org/10.1016/j.jcmg.2018.02.022

ABBREVIATIONS AND ACRONYMS

ACR = acute cellular rejection

CAV = cardiac allograft vasculopathy

CI = confidence interval

CMR = cardiac magnetic resonance

ECV = extracellular volume

EF = ejection fraction

EMB = endomyocardial biopsy

GCS = global circumferential strain

GLS = global longitudinal strain

grade 1R = grade 1 rejection

grade 2R = grade 2 rejection

HTx = heart transplantation

NPV = negative predictive value

Acute allograft rejection remains a major issue for heart transplantation (HTx) patients (1). Timely treatment is indispensable to avoid allograft loss. Endomyocardial biopsy (EMB) remains the gold standard for diagnosing rejection, despite considerable limitations. In addition, acute rejections are now more silent and difficult to detect thanks to improvements in immunosuppressive treatments. As the risk for acute rejection has decreased over the years (2), the number of unnecessary biopsies has increased. Noninvasive alternatives are highly desirable to monitor allograft rejection.

SEE PAGE 1615

Although echocardiography is the primary imaging modality for follow-up, conventional functional and morphological parameters are known to be insensitive markers of cardiac allograft rejection. Because of patchy distribution of acute cellular rejection (ACR), the combination of structural and functional imaging with full coverage of left ventricle may help overcome the limited information of conventional parameters (3–5). Therefore, we hypothesized that characterization and quantification of myocardial tissue properties by cardiac magnetic resonance (CMR) T1 mapping and mechanical alterations by echocardiographic speckle-tracking strain are complementary to each other and can provide valuable noninvasive indexes to detect ACR in HTx patients.

METHODS

In the first part of the study, we retrospectively reviewed surveillance EMBs, catheterization findings, and echocardiograms of HTx patients obtained serially according to our institutional protocol since transplantation (from January 2009 to January 2016). After January 2016, we decided to add CMR to the surveillance protocol and conducted the second, cross-sectional part of the study, including CMR irrespective of patient symptoms. All tests were done within 48 h of each other on consecutive patients. In the first part, 49 of 64 adult HTx patients were included consecutively. Excluded patients underwent HTx <1 month previously (n = 3) and had

FIGURE 1 Flow Diagram of the Study

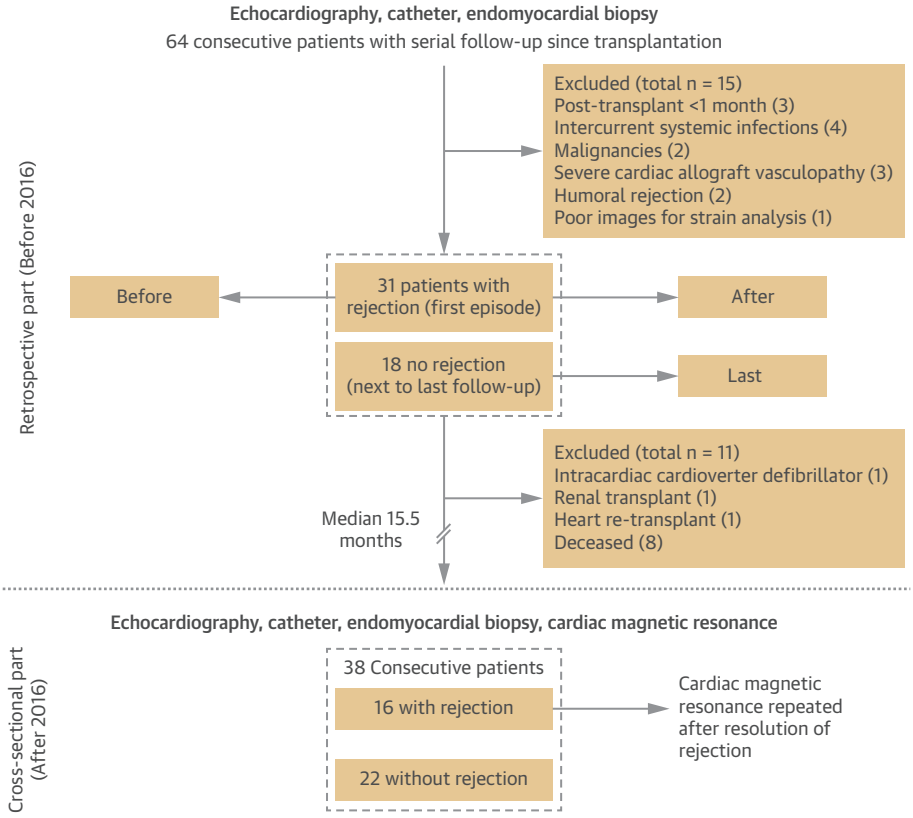

FIGURE 2 Speckle-Tracking Strain and T1 Quantification

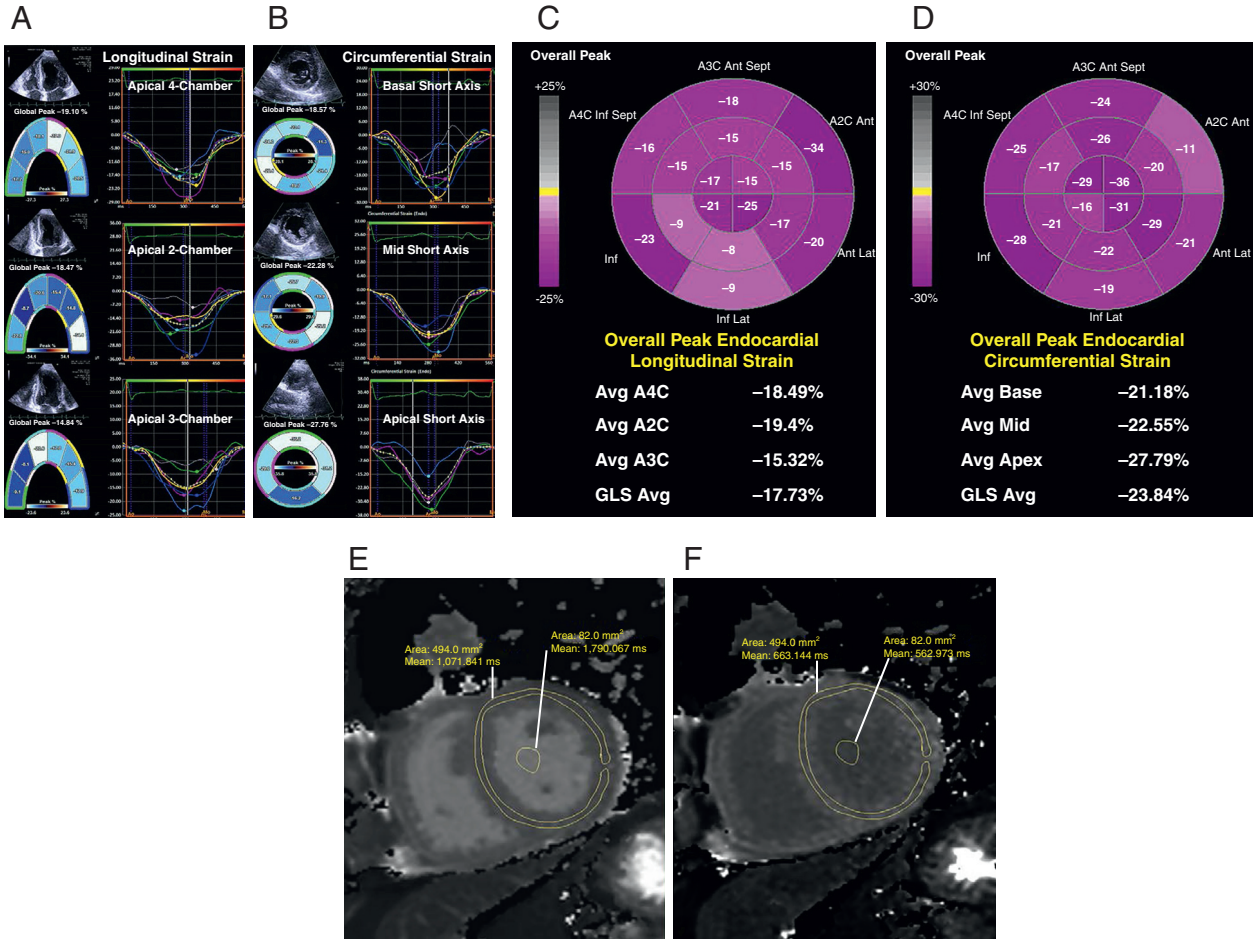

Apical **(A)** and short-axis **(B)** views and corresponding segmental time-strain curves and bull's-eye maps of longitudinal **(C)** and circumferential **(D)** strain. T1 map images with identical regions of interest covering all midventricular segments, two-thirds of central wall thickness, and another placed at the center of the cavity on pre-contrast **(E)** and post-contrast **(F)** images. A2C = apical 2-chamber; A3C = apical 3-chamber; A4C = apical 4-chamber; GCS = global circumferential strain; GLS = global longitudinal strain.

intercurrent systemic infections (n = 4), malignancies (n = 2), severe cardiac allograft vasculopathy (CAV) (n = 3), humoral rejection (n = 2), or poor images for strain analysis (n = 1). The first rejection episode was counted as the index event. Strain was measured at 3 time points in patients with rejection (before, during, and resolution of rejection) and at 2 time points for patients without rejection (most recent and preceding) (Figure 1). In the first part, we assessed the potential of strain quantification for detecting ACR. The second cross-sectional part of the study, with CMR, served to validate previously derived strain cutoffs, examine the progression of strain over time, and test the accuracy of T1 mapping, with a head-to-head comparison with strain, to detect ACR. All patients had glomerular filtration rates >35 ml/min/1.73 m^2.

The study protocol was approved by the Institutional Review Board and Institutional Ethical Committee for Human Research of Baskent University and complied with the Declaration of Helsinki. All patients gave informed consent.

Pressure measurements were performed during EMB procedures invasively. Coronary angiography early after transplantation to detect donor-related coronary artery disease and yearly thereafter to detect CAV was also part of our follow-up protocol.

EMB. EMB is performed at 1, 2, 4, 6, and 10 weeks, 6 and 12 months, and yearly thereafter at our institution. Additional biopsies are performed whenever rejection is suspected or to confirm treatment success. ACR is determined on the basis of the severity of inflammatory infiltrates and myocyte damage

TABLE 1 Baseline Clinical Characteristics

	Rejection (n = 31)	No Rejection (n = 18)	p Value
Donor age, yrs	28 (22–42)	30 (25–35)	0.60
Recipient age, yrs	46 (32–52)	34 (20–39)	0.005
Women	10 (32)	6 (33)	0.90
Time from transplantation, months	3 (3–36)	12 (36–84)	0.0001
Hypertension	9 (29)	6 (33)	0.75
Fasting glucose, mg/dl	98 (93–107)	94 (88–98)	0.06
Creatinine, mg/dl	0.88 (0.81–1.09)	0.85 (0.74–1.03)	0.65
Systolic blood pressure, mm Hg	120 (110–130)	118 (105–130)	0.19
Diastolic blood pressure, mm Hg	80 (70–80)	80 (70–80)	0.68
Body mass index, kg/m^2	1.83 (1.73–1.94)	1.75 (1.63–1.87)	0.13
Corticosteroid	29 (93)	17 (94)	0.50
Mycophenolate mofetil	30 (97)	18 (100)	0.44
Tacrolimus	21 (68)	7 (39)	0.19
Sirolimus	10 (32)	4 (22)	0.59

Values are median (interquartile range) or n (%).

according to the standardized International Society for Heart and Lung Transplantation nomenclature (6).

ECHOCARDIOGRAPHY. Standard 2-dimensional echocardiography was performed by using the SC 2000 cardiac ultrasound machine (Siemens Medical Solutions USA, Mountain View, California) according to our protocol (7). This protocol also includes yearly performed dobutamine stress echocardiography for assessing CAV (7). We reviewed echocardiograms obtained concomitantly with EMBs. Speckle-tracking strain analyses were performed from 3 cine loops, digitally stored at a frame rate of 40 to 90 frames/s, using a dedicated software (Velocity Vector Imaging, Siemens Healthcare, Erlangen, Germany). Curved regions of interest were manually traced on the endocardial border in apical 4-chamber, 2-chamber, long-axis, and basal, mid, and apical short-axis views. Regional strain was calculated by automated tracking of the location shifts of the acoustic markers in the endocardium. All image planes were divided into 6 segments and only the apical short-axis image into 4 segments, automatically. Global longitudinal strain (GLS) was obtained from 3 apical views and global circumferential strain (GCS) from 3 short-axis planes, as the average of the means of each plane (**Figures 2A to 2D**).

CMR. CMR was performed using a 1.5-T scanner (Ingenia CX, Philips Healthcare, Best, the Netherlands). Cine images were obtained using a short-axis cine steady-state free precession sequence. T1 measurements were performed using modified Look-Locker inversion recovery pulse sequence images that were acquired in short-axis slices covering the whole ventricle, during a breath hold, before and 15 min after the administration of 0.2 mmol/kg gadoterate meglumine (Dotarem, Guerbet, Villepinte, France). This acquisition sampled the inversion recovery using a 5s(3s)3s scheme for native T1 and a 4s(1s)3s(1s)2s scheme following contrast. Parameters were field of view 300 × 300 mm, matrix size 152 × 150, resolution 1.97 × 2 mm, slice thickness 10 mm, repetition time 2 ms, echo time 0.91 ms, flip angle 35°, acquisition window 188 ms, parallel imaging factor 2, partial echo factor 0.85, and minimum inversion time for pre-contrast scan 120 ms and for post-contrast scan 140 ms. Normal native T1 values of the scanner were between 967 and 1,029 ms. Late gadolinium hyperenhancement images were obtained using a

TABLE 2 Echocardiographic and Hemodynamic Findings Before and During Rejection and in Patients With No Rejection

	Grade 1 Rejection (n = 16)		Grade ≥2 Rejection (n = 15)		No Rejection (n = 18)
	Before	R1 Rejection	Before	R2 Rejection	
GLS, %	−18.3 (−20.7 to −17.2)	−16.7 (−18.4 to −14.9)*	−18.4 (−21.0 to −17.3)	−14.0 (−16.6 to −12.4)†	−18.9 (−22.1 to −16.8)‡¶
GCS, %	−28.9 (−34.0 to −23.4)	−24.0 (−26.2 to −21.0)*	−27.2 (−34.3 to −26.0)	−20.4 (−28.0 to −15.6)†	−29.0 (−33.4 to −24.0)‡‖
EF, %	58 (56 to 61)	58 (52 to 60)	58 (54 to 62)	56 (53 to 59)	60 (55 to 60)
EDV, ml	74 (70 to 85)	81 (75 to 89)	75 (70 to 104)	90 (69 to 114)	80 (66 to 92)
ESV, ml	34 (30 to 35)	33 (30 to 42)	36 (29 to 46)	37 (32 to 46)	35 (28 to 41)
TAPSE, mm	14 (12 to 17)	15 (13 to 18)	14 (12 to 16)	13 (10 to 15)*	16 (15 to 18)§
S, cm/s	8.5 (8.0 to 9.1)	8.0 (7.3 to 9.1)	8.7 (8.3 to 9.7)	8.8 (7.0 to 9.5)	9.2 (7.0 to 10.5)
E, cm/s	10.5 (10.0 to 12.0)	11.5 (9.7 to 13.3)	11.6 (10.6 to 12.7)	10.5 (9.2 to 13.6)	11.4 (10.5 to 13.8)
Cardiac index, l/m^2	2.8 (2.7 to 2.9)	2.7 (2.3 to 3.0)	2.6 (2.5 to 2.9)	2.5 (2.1 to 3.3)*	3.2 (2.3 to 3.6)
sPAP, mm Hg	26 (21 to 32)	26 (24 to 29)	28 (24 to 34)	31 (27 to 39)	26 (22 to 28)‡
PCWP, mm Hg	12 (9 to 14)	13 (10 to 15)	13 (10 to 17)	16 (10 to 19)	11 (8 to 13)§
RAP, mm Hg	5 (4 to 8)	4 (3 to 6)	6 (3 to 7)	8 (6 to 9)*	5 (4 to 8)§

Values are median (interquartile range). *p < 0.05 versus before. †p < 0.01 versus before. ‡p < 0.001 versus R2 rejection. §p < 0.05 versus R2 rejection. ‖p < 0.01 versus R1 rejection. ¶p < 0.05 versus R1 rejection.

E = early diastolic mitral inflow velocity; EDV = end-diastolic volume; EF = ejection fraction; ESV = end-systolic volume; GCS = global circumferential strain; GLS = global longitudinal strain; PCWP = pulmonary capillary wedge pressure; RAP = right atrial pressure; sPAP = systolic pulmonary artery pressure; S = mitral annular (average septal and lateral) systolic velocity; TAPSE = tricuspid annular peak systolic excursion.

phase-sensitive inversion recovery segmented gradient echo sequence 10 min after gadolinium administration in 2 long- and short-axis planes. T1 analyses were performed using dedicated Cardiac Quant software (Philips Healthcare). After controlling for motion artifacts, regions of interest were manually traced at the basal and midventricular short-axis slices, and measurements were averaged, excluding areas enhanced on late gadolinium hyperenhancement images to avoid partial volume effects, on the left ventricular wall and center of the left ventricular cavity (Figures 2E and 2F). Extracellular volume (ECV) was calculated as: myocardial ECV = (1 − hematocrit) × (ΔR1 myocardium/ΔR blood), where R1 = 1/T1 (8).

STATISTICAL ANALYSIS. SPSS version 18 (SPSS, Chicago, Illinois) was used. Data are expressed as numbers and percentages or as medians and interquartile ranges. Mann-Whitney *U*, Wilcoxon signed rank, and Friedman tests for related groups and the Kruskal-Wallis H test for independent groups were used to determine differences. Chi-square or Fisher exact tests were used for categorical variables. Univariate logistic regression analysis was performed for potential determinants of rejection. Parameters with p values <0.10 in the univariate analysis were entered into a multivariate logistic regression model with forward selection. Cutoffs were defined from receiver-operating characteristic curves by using the maximum Youden index. All analyses investigating the predictive efficiency of specific thresholds of T1 and GLS included only 1 rejection episode of the patient to avoid the confounding that may be introduced by correlated longitudinal observations. Intraobserver and interobserver reliabilities of GLS, GCS, and T1 time were described using intraclass correlation coefficients (2-way mixed effects, absolute agreement, single measure). Two-tailed p values <0.05 were considered to indicate statistical significance.

FIGURE 3 Global Longitudinal Strain and Global Circumferential Strain According to Rejection Status

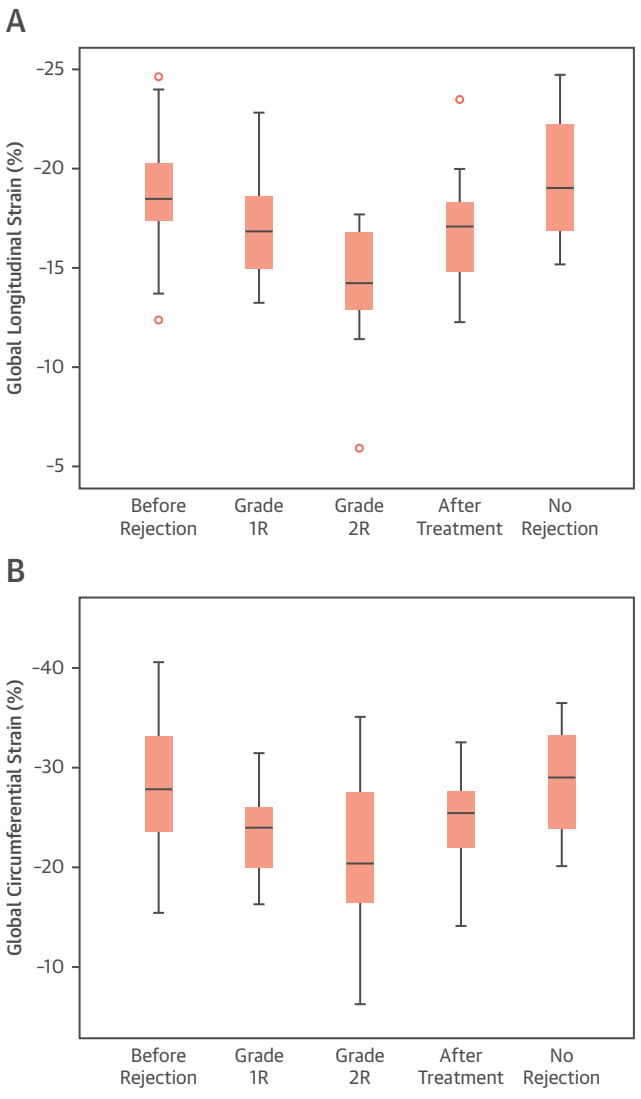

Note the impairment in global longitudinal strain **(A)** and global circumferential strain **(B)** during rejection and no complete normalization after treatment.

RESULTS

PART 1. Of 49 patients, the first rejection episode was grade 1 rejection (grade 1R) in 16, grade 2 rejection (grade 2R) in 14, and grade 3 rejection in 1 patient. Eighteen patients had no rejection (Table 1). Table 2 presents the echocardiographic findings in patients with (before and during) and without rejection. Only GLS and GCS reduced significantly during grade 1R. During grade ≥2R, GLS, GCS, tricuspid annular peak systolic excursion and cardiac index reduced and right atrial pressure increased significantly. Measurements before rejection were not different from measurements in the no-rejection group. GLS and GCS improved significantly only after treatment of grade ≥2R (GLS from −14.0% [16.6% to −12.4%] to −17.9% [−19.8% to −16.7%], p = 0.04; GCS from −20.4% [−28.0% to −15.6%] to −25.5% [−30.9% to −21.7%], p = 0.02). Overall, despite successful treatment, strain values did not reach exactly the pre-rejection levels and remained significantly worse than the values in the no-rejection group (GLS −17.0%

FIGURE 4 Changes in Global Longitudinal Strain With Rejection

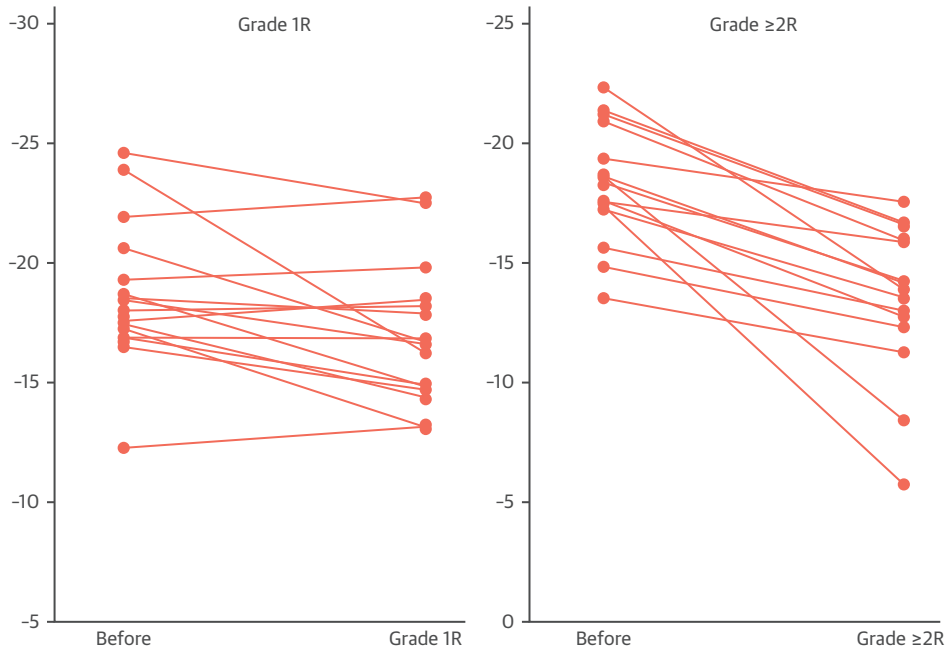

Grade 1R **(A)** and grade ≥2R **(B)**. Global longitudinal strain worsened in every patient with grade ≥2R.

[−18.3% to −14.7%] vs. −18.9% [−22.1% to −16.8%], p = 0.006; GCS −25.5% [−27.8% to −22%] vs. −29.0% [−33.4% to −24.0%], p = 0.01) (Figure 3). Importantly, GLS decreased in every patient (100%) during grade ≥2R and in 11 of 16 patients (69%) during grade 1R (Figure 4).

GLS and GCS determined grade ≥2R and also grade 1R. Their best fit cutoff values are presented in Figure 5. In the multivariate logistic regression analysis including the most pertinent variables (tricuspid annular plane systolic excursion, cardiac index, right atrial pressure, and recipient age) according to univariate analyses, GLS and GCS emerged as independent determinants of any rejection (p = 0.015 and p = 0.004, respectively). Time delay from transplantation was significantly shorter in patients with rejection, as expected (9), and therefore was not included in the multiple regression model.

PART 2. Part 2 was conducted 15.5 months (interquartile range: 12 to 24 months) later with 38 consecutive patients after exclusion of those with intracardiac defibrillator (n = 1), renal transplantation (n = 1), and re-HTx (n = 1) and those who died (n = 8, 4 from systemic infections, 2 from malignancies, 2 from rejection).

There were 10 episodes of grade 1R and 6 episodes of grade 2R. The cutoff values derived from the first part had higher sensitivity but lower specificity (GLS −17%: sensitivity 82%, specificity 50%; GCS −26%: sensitivity 77%, specificity 53%) to detect any rejection, because at that time, the best cutoffs were less negative than those defined in the first part (GLS −16% and −14% and GCS −25% and −24% for grades 1R and 2R, respectively). An explanation was the decremental course of strain over time in patients who survived previous rejections, despite resolution, in contrast to almost stable strain in patients who survived no rejection (Figure 6).

CMR data are presented in Table 3 and Figure 7. T1 time and ECV were significantly reduced during grade 1R and 2R. Furthermore, T1 time was the only independent determinant of grade 1R, while GLS and T1 time were independent determinants of grade 2R (Table 4). Cutoffs, sensitivities, specificities, negative predictive value (NPV), and positive predictive value for T1 time and strain are presented in Table 5 and Figure 8. T1 time ≥1,060 ms had 82% sensitivity and 86% NPV to define grade 1R. Its sensitivity increased to 91% and its NPV to 92% when combined with GLS >−16%. To

FIGURE 5 Receiver-Operating Characteristic Curves for Accuracy to Define Acute Cellular Rejection by GLS and GCS

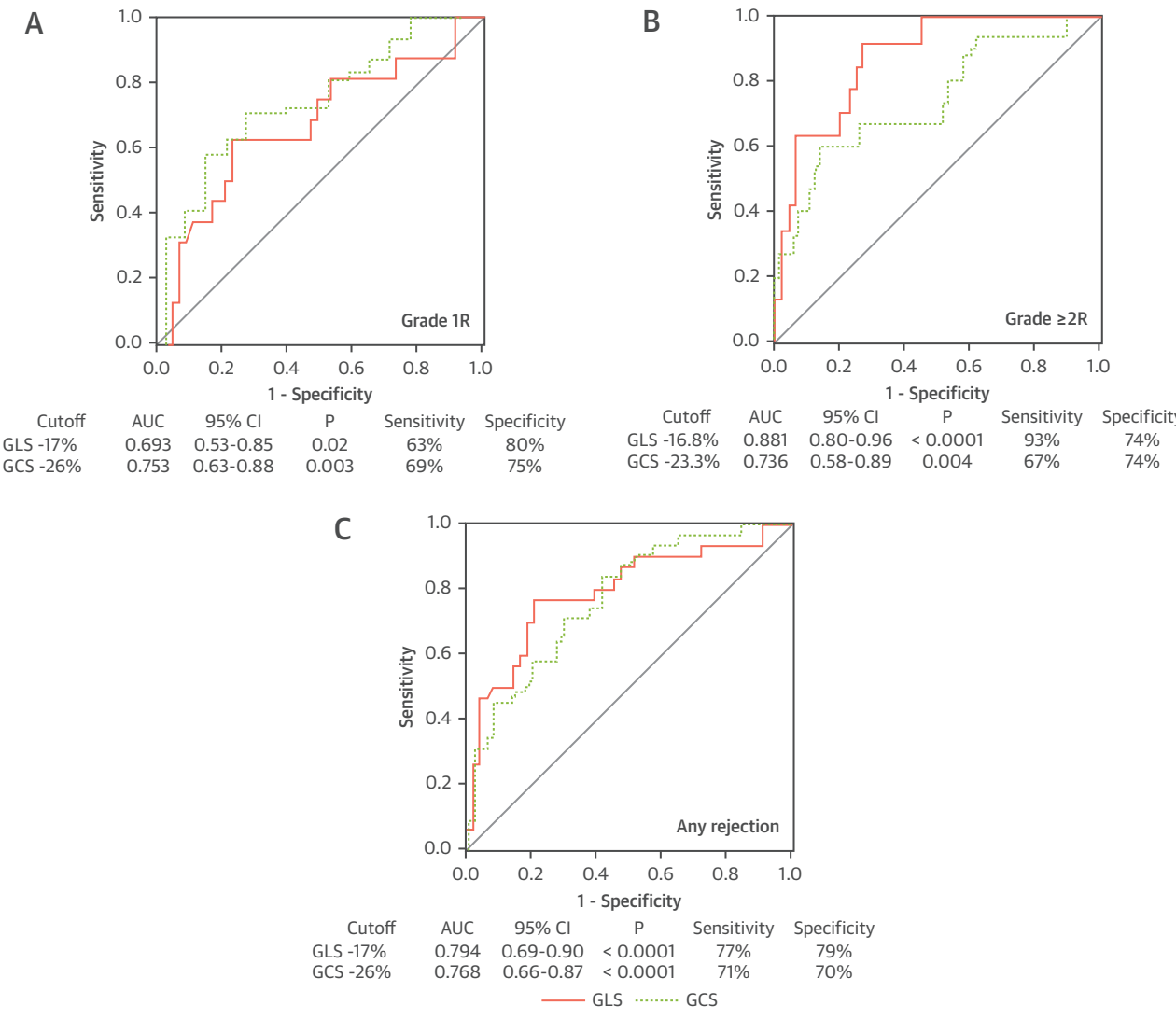

Grade 1R **(A)**, grade ≥2R **(B)**, and any rejection **(C)**. AUC = area under the curve; CI = confidence interval; GCS = global circumferential strain; GLS = global longitudinal strain.

determine grade 2R, T1 time (cutoff ≥1,090 ms), ECV (cutoff ≥32%), GLS (cutoff >−14%), and GCS (cutoff ≥−24%) had 100% sensitivity and 100% NPV. Patients with rejection underwent repeat CMR 3 months later if resolution of rejection was confirmed by EMB. T1 time decreased from 1,105 ms (1,054 to 1,141 ms) to 1,085 ms (1,051 to 1,096 ms) (p = 0.02), but the decrease in ECV did not reach statistical significance. Importantly, T1 time after resolution tended to be higher than in the no-rejection and never-rejected groups (Figure 7).

Intraobserver and interobserver intraclass correlation coefficients, calculated in 10 patients, were 0.985 (95% confidence interval [CI]: 0.942 to 0.996) and 0.947 (95% CI: 0.769 to 0.987) for T1 time, 0.975 (95% CI: 0.836 to 0.994) and 0.978 (95% CI: 0.919 to 0.994) for GCS, 0.975 (95% CI: 0.670 to 0.994), and 0.964 (95% CI: 0.868 to 0.991) for GLS, respectively.

FIGURE 6 Global Longitudinal Strain and Global Circumferential Strain Over Time in Patients With and Without Rejection

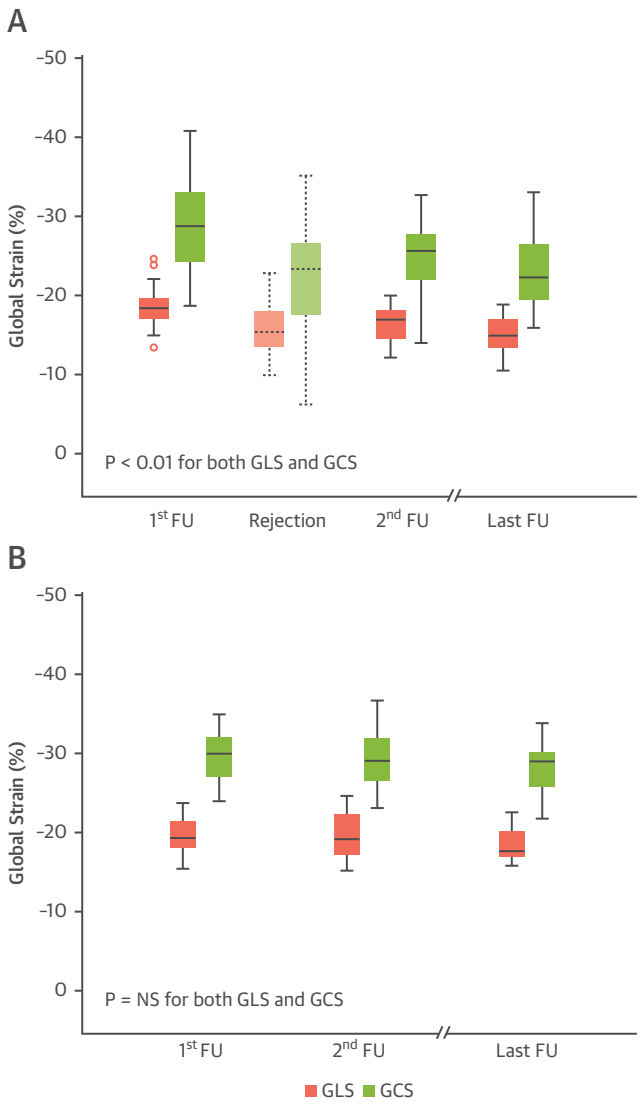

Note the significant decreases in global longitudinal strain (GLS) and global circumferential strain (GCS) in patients who survived rejection **(A)** and almost stable GLS and GCS in patients who survived no rejection **(B)**. FU = follow-up; NS = nonsignificant.

DISCUSSION

Our main findings are as follows: 1) CMR T1 mapping and echocardiographic GLS are reliable to define grade ≥2R ACR and complementary to each other to define grade 1R in HTx patients; 2) a decrease in GLS is a unanimous finding during grade ≥2R despite preserved ejection fraction (EF); 3) there is no complete return to baseline values after resolution of grade ≥2R, and a smoldering deterioration of the graft over the years, that can be quantified by strain; and 4) strain cutoffs to determine ACR are time dependent.

Several single-center studies compared CMR findings with EMB for allograft rejection, T2 imaging being the most widely used technique. Significant increase in absolute T2 values or relative T2 signal intensity were reported in relation to ACR (10,11). Lately, the prolongation of T2 relaxation time, as a quantitative means of assessing myocardial edema (12), has provided more reproducible results and determined grade ≥2R better (3,4,13). In contrast, late gadolinium hyperenhancement as a means of quantifying myocardial fibrosis was not found to correlate with ACR, likely because of the small size of areas with myocyte necrosis related to rejection (3,11,14) and its inability to differentiate old from new fibrosis, even if ACR-related fibrosis is different from infarct typical hyperenhancement (14). Combining structural and functional information to better define myocardial damage related to rejection has also been previously suggested (3,4). Markl et al. (4) assessed the relationship between myocardial velocity and T2 relaxation times, and Butler et al. (3) combined T2 relaxation times and right ventricular function by CMR to detect grade ≥2 rejection in HTx patients.

Data on T1 imaging for monitoring ACR in HTx patients are scarce (15). T1 signal intensity had limited reproducibility and yielded inconsistent results. However, preliminary quantitative T1 data were promising (16,17). Although T2 times are more reflective of water content, native T1 times and ECV have the advantage of reflecting extracellular expansion including not only fibrosis but also edema and inflammation (18), which are typical features of ACR depending on its severity. Obviously, fibrosis may result from CAV, but we used not only angiography but also dobutamine stress echocardiography to exclude CAV (7). Therefore, T1 time prolongation and ECV augmentation in our population are a reflection of ACR rather than CAV-related fibrosis. We also found that prolonged T1 times resolved after intensification of immunosuppressive treatment, further supporting our hypothesis.

GLS has gained considerable importance as a reproducible and sensitive quantification tool for myocardial function lately, in a variety of diseases and also in patients who undergo HTx (19). Speckle-tracking strain and CMR enable the assessment of the entire myocardium and therefore could be more sensitive than biopsy to detect ACR. We used a 16-segment model with strain and the entire

TABLE 3 Cardiac Magnetic Resonance Findings in Patients With and Those Without Rejection

	No Rejection* (n = 11)	R1 Rejection (n = 10)	R2 Rejection (n = 6)	Never Rejected† (n = 11)
T1 time, ms	1,075 (1,049–1,094)	1,096 (1,060–1,143)‡§	1,132 (1,111–1,134)‡‖	1,035 (1,007–1,052)
ECV, %	30.0 (28.0–33.4)	34.8 (31.0–36.6)¶#	35.0 (33.0–38.9)‡‖	27.7 (25.7–29.0)
EF, %	68.1 (64.0–73.1)	65.6 (63.0–72.8)	55.4 (52.0–62.0)‡‖	67.2 (64.0–73.0)
EDVI, ml/m^2	77.2 (67.0–80.2)	73.5 (65.0–88.7)	72.7 (69.0–80.0)	71.0 (62.5–81.0)
ESVI, ml/m^2	24.5 (21.6–26.4)	27.1 (23.0–37.0)¶	28.4 (22.0–39.0)	25.0 (24.0–31.5)
SVI, ml/m^2	27.7 (26.8–30.9)	29.5 (25.0–34.0)	23.6 (21.6–26.4)	26.6 (21.3–31.5)
LVMI, g/m^2	62 (50–73)	68 (53–76)	65 (58–81)	59 (49–70)
LGE**	3 (2–3)	2 (1–3)	3 (2–4)	2 (1–3)

Values are median (interquartile range). *Patients without rejection at the time of surveillance. †Patients without rejection at the time of surveillance and without rejection in the past since transplantation. ‡$p < 0.01$ versus never rejected. §$p < 0.01$ versus combined no rejection and never rejected. ‖$p < 0.05$ versus no rejection. ¶$p < 0.05$ versus never rejected. #$p < 0.05$ versus combined no rejection and never rejected. **Number of segments with LGE.

ECV = extracellular volume; EDVI = end-diastolic volume index; EF = ejection fraction; ESVI = end-systolic volume index; LGE = late gadolinium hyperenhancement; LVMI = left ventricular mass index; SVI = stroke volume index.

circumference of the left ventricle by T1 quantification. Biopsy-negative rejection is well recognized (20,21). Therefore, ACR cannot be excluded in all patients with abnormal imaging findings and no evidence of rejection on biopsy, because random and limited biopsy sampling can miss patchy foci of rejection. This partly explains the relatively low positive predictive value of imaging in comparison with EMB as a reference. Also, in the study of Marie et al. (10), patients with CMR results defined as false positive were significantly more likely to develop rejection in the subsequent 3 months than those with normal results on CMR and EMB.

We observed that GLS tracked functional deterioration during ACR more accurately than GCS. Clemmensen et al. (19) also showed that GLS, but not GCS, correlated with ACR. However, they assessed circumferential strain at the mid left ventricular level only, while we assessed in all 3 short-axis planes to better represent the entire left ventricle. Indeed, our study is the first to assess the entire left ventricle with multidimensional strain in comparison with concomitant EMB and CMR in HTx patients. Importantly, we also observed a wide range of "normal" strain values in our HTx patients in the absence of rejection, which is in accordance

FIGURE 7 T1 Relaxation Time and Extracellular Volume According to Rejection Status

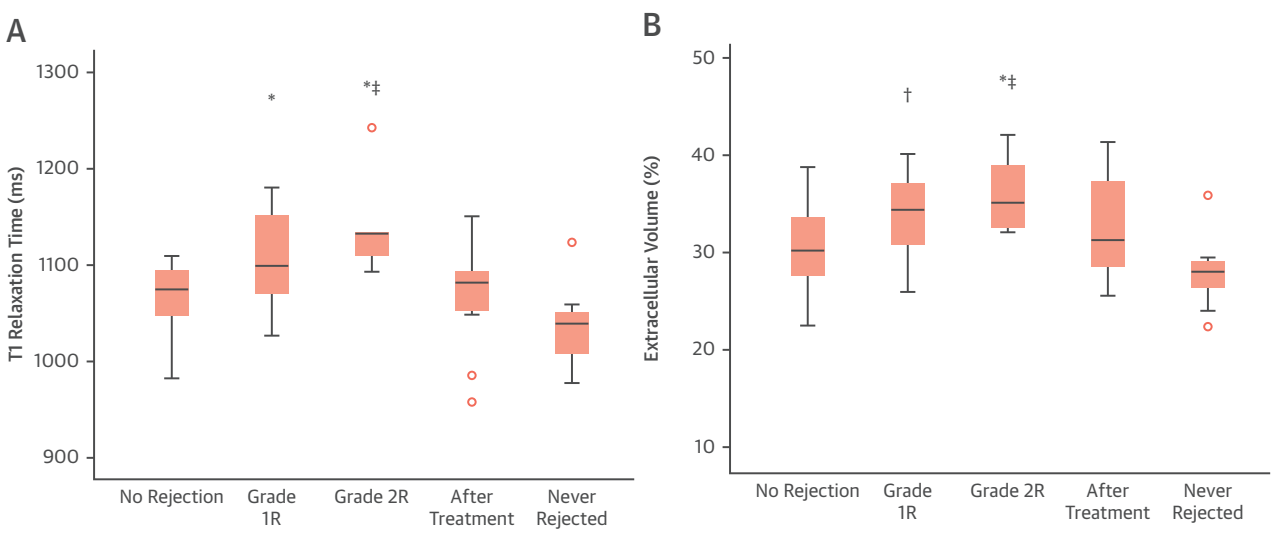

T1 time **(A)** and extracellular volume **(B)** increased significantly in comparison with the never-rejected group during grade 1R and 2R and in comparison with the no-rejection group during grade 2R. *$p < 0.001$ versus never rejected, †$p < 0.05$ versus never rejected, ‡$p < 0.05$ versus no rejection.

TABLE 4 Univariate and Multivariate Determinants of Grade 1 Rejection and Grade 2 Rejection

	Grade 1 Rejection				Grade ≥2 Rejection			
	Univariate		Multivariate		Univariate		Multivariate	
	p Value	95% CI	p Value	95% CI	p Value	95% CI	p Value	95% CI
Age	0.23	0.97–1.12			0.21	0.86–1.03		
Fasting glucose	0.29	3.09–5.94			0.4	0.04–3.69		
EF*	0.91	0.88–1.14			0.04	0.687–0.987	–	–
TAPSE	0.05	0.455–1.992	–	–	0.03	0.211–0.829	–	–
GLS	0.28	0.62–1.15			0.03	0.616–0.984	0.03	0.100–0.909
GCS	0.52	0.37–6.82			0.50	0.86–1.07		
PCWP	0.14	0.96–1.37			0.20	0.94–1.39		
sPAP	0.17	0.96–1.23			0.39	0.94–1.17		
Cardiac index	0.70	0.43–3.47			0.25	0.03–2.52		
RAP	0.04	1.046–3.298	–	–	0.16	0.99–1.56		
T1 time	0.01	1.006–1.053	0.02	1.002–1.056	0.02	1.003–1.042	0.02	1.014–1.194
ECV†	0.02	1.047–1.606			0.04	1.10–1.558		

*By echocardiography. †ECV was not included in the multivariate analysis to avoid collinearity with T1 time.
CI = confidence interval; other abbreviations as in Tables 2 and 3.

with previous findings (20,22). As a result, different cutoff values have been reported to define grade ≥2 rejection in various studies (19,23,24). Furthermore, our findings underline that cutoffs are time dependent because of the continuous remodeling process in transplanted hearts. In addition, after resolution of rejection, left ventricular strain does not completely return to baseline values, consistent with previous studies (19). Hence, it is difficult to define generalizable cutoffs of strain to define the early phase of allograft rejection. Serial follow-up with GLS, a sensitive index of myocardial function, seems rather reasonable to detect ACR noninvasively.

Of note, HTx patients without rejection had slightly lower GLS than that observed in healthy subjects. Attenuated GLS has already been shown compared with healthy control subjects at all times after transplantation (22,25,26). This is valid also for "normal" T1 and T2 times after HTx (4,14). Even stable HTx patients demonstrate subclinical structural and functional alterations due to remodeling within the transplanted heart (27). Several causes could be the reason of the insidious graft remodeling over the long term, including surgical trauma, ischemia, transport damage, undetected smoldering rejection, rejection-resolution episodes, infections, sympathetic denervation, immunosuppressive agents, and CAV at the micro- and macrovascular levels. Not only grade ≥2R but also grade 1R leads to impaired longitudinal deformation over the long term (28). Our nonrejecting patients had GCS values that were comparable with those in healthy subjects, however. This is also in keeping with previous studies (26), most likely because longitudinal function reflects early and subtle myocardial dysfunction when GCS compensates and maintains the EF. No significant change in EF during mild rejection is in accordance with previous data (13,15). We found EF to be a univariate predictor of grade 2R but not 1R. Conventional functional and morphological measures such as reduced EF, pericardial effusion, and increased wall thickness are late manifestations of rejection and therefore not suitable for screening. Preservation of GCS during mild damage also helps maintain EF until late in the course of rejection.

Feature tracking approaches allow easy measurement of GLS using cine CMR images as well. Although the versatile use of CMR is attractive, the repetition

TABLE 5 Accuracy of Strain and T1 Time Alone or in Combination to Determine Rejection

	Sensitivity	Specificity	NPV	PPV	Cutoff
Grade 1 rejection					
T1 time	82%	74%	86%	63%	≥1,060 ms
ECV	82%	68%	80%	60%	≥30%
GLS	55%	74%	74%	55%	>−16%
GCS	58%	65%	69%	54%	>−25%
T1/GLS	91%	58%	92%	56%	1,060/−16
Grade ≥2 rejection					
T1 time	100%	73%	100%	70%	≥1,090 ms
ECV	100%	63%	100%	63%	≥32%
GLS	100%	83%	100%	55%	>−14%
GCS	100%	62%	100%	35%	≥−24%

NPV = negative predictive value; PPV = positive predictive value; other abbreviations as in Tables 2 and 3.

FIGURE 8 **Receiver-Operating Characteristic Curves for Accuracy to Define Rejection by T1 Time and Extracellular Volume**

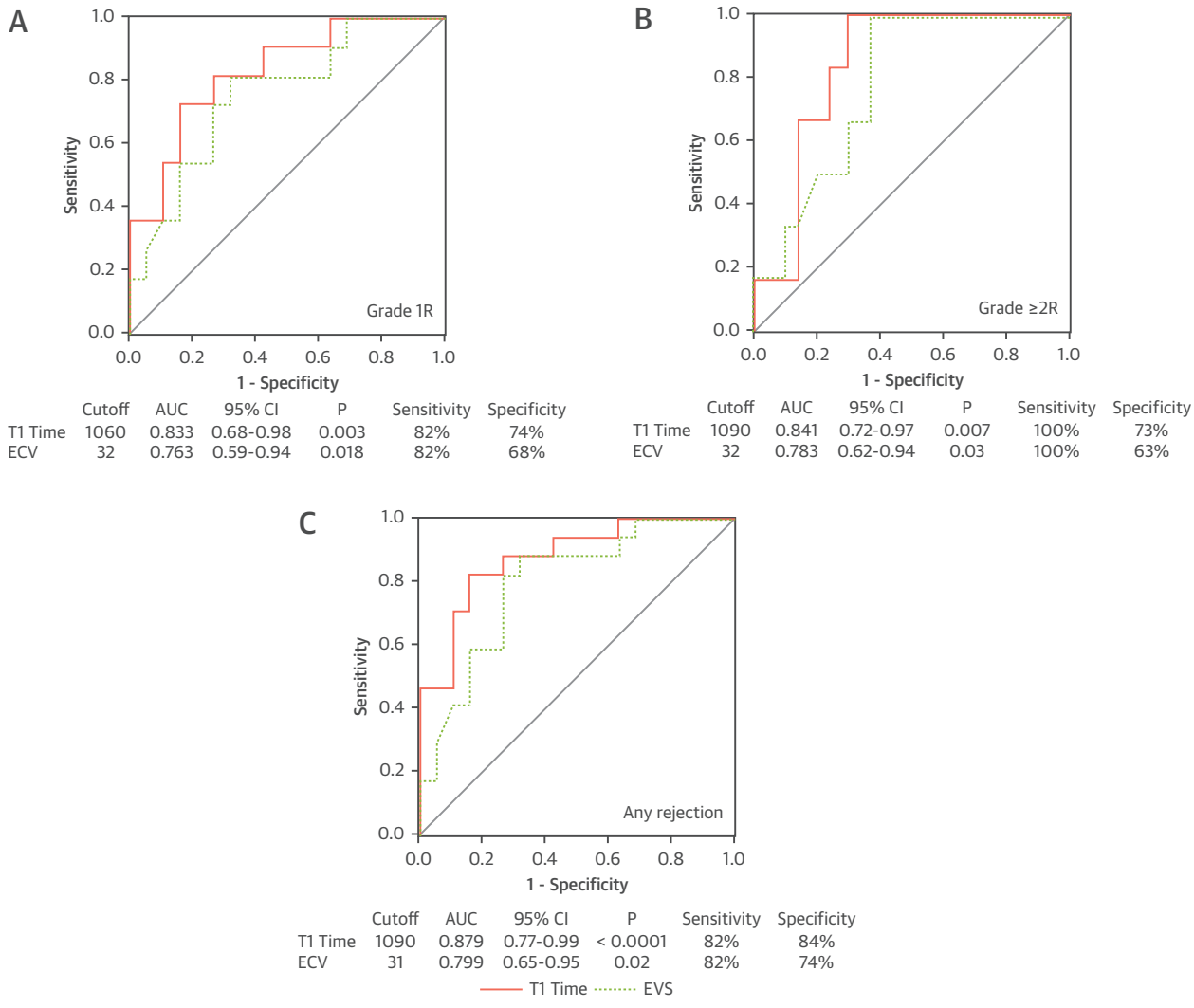

	Cutoff	AUC	95% CI	P	Sensitivity	Specificity
T1 Time	1060	0.833	0.68-0.98	0.003	82%	74%
ECV	32	0.763	0.59-0.94	0.018	82%	68%

	Cutoff	AUC	95% CI	P	Sensitivity	Specificity
T1 Time	1090	0.841	0.72-0.97	0.007	100%	73%
ECV	32	0.783	0.62-0.94	0.03	100%	63%

	Cutoff	AUC	95% CI	P	Sensitivity	Specificity
T1 Time	1090	0.879	0.77-0.99	< 0.0001	82%	84%
ECV	31	0.799	0.65-0.95	0.02	82%	74%

Grade 1R **(A)**, grade 2R **(B)**, and any rejection **(C)**. Abbreviations as in previous figures. AUC = area under the curve; CI = confidence interval; ECV = extracellular volume.

frequency to track subtle myocardial functional alterations needs to be explored in order to balance cost and potential harm as a screening test to replace echocardiographic strain quantification.

CLINICAL IMPLICATIONS. Our results extend previous findings by incorporating imaging for myocardial function and tissue characteristics to detect cardiac allograft rejection noninvasively. GLS and T1 time alone had very high NPV to rule out grade ≥2R and very high sensitivity to screen patients for grade ≥2R. Furthermore, the combination of GLS and T1 time provided reasonable accuracy to track mild ACR (grade 1R), which can help fine-tune immunosuppressive therapy before waiting for manifest rejection episodes. We suggest a strategy of noninvasive monitoring for ACR, as illustrated in **Figure 9**, to risk-stratify patients and possibly defer unnecessary biopsies. In particular, up to 2 years after transplantation, to rule out rejection confidently, we underline the importance of serial GLS comparisons. Any decrease in GLS, particularly during this period, should be regarded as possible rejection, because in patients without CAV or rejection, the graft deterioration is insidious, and overall GLS is expected to remain stable as long as the patient stays "healthy" (29). Because CMR data were

FIGURE 9 Global Longitudinal Strain and T1 Mapping to Risk-Stratify Patients for Acute Cellular Rejection

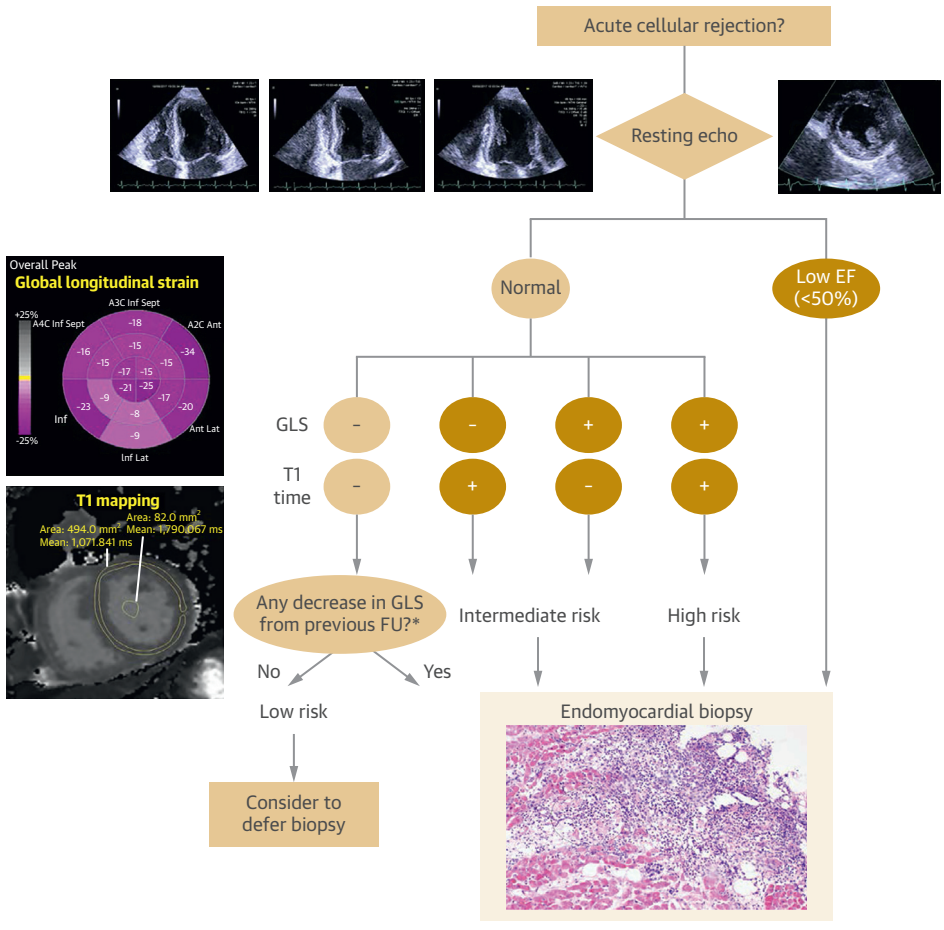

Endomyocardial biopsy may be deferred if global longitudinal strain (GLS) ≤−16%, T1 time <1,060 ms, and no decrement in GLS in comparison with previous follow-up are confirmed (*particularly first 2 years post-transplantation). EF = ejection fraction; FU = follow-up.

obtained later than the first year after transplantation in the present study, whether the T1 time cutoffs can be extended to the first year after transplantation needs to be further tested.

STUDY LIMITATIONS. Despite a relatively small patient population, our results represent an unselected cohort with routine follow-up tests, unlike most published studies that investigated the role of noninvasive ACR surveillance techniques in selected patients with suspected ACR and usually outside the time period when the early detection of ACR is likely to be most useful. The second part of our study, including CMR, was conducted later in time. This is also probably not a severe limitation because quantitative "normal" T1 and T2 measurements were found to be higher after transplantation compared with healthy volunteers and improved over time (16), suggesting that CMR parameters become more useful and stable for detecting ACR as time from transplantation increases. We excluded patients immediately after the operation (first month) because myocardium is affected by operation-related conditions in this time period, diminishing the accuracy of imaging for rejection (18). Our results cannot be extrapolated to patients with humoral rejection. To avoid the confounding that may be introduced by the correlated observations potentiating the effect of the predictive value of T1 mapping and strain cutoffs, we included only 1 rejection per patient in each part of the study. Yet from the clinical perspective, there is no reason to think that the highly discriminatory capacity of these tests will vanish for repeated evaluations of rejections. Minor deviations in hematocrit levels cannot be excluded as a potential source of

error for the calculation of ECV, as blood samples were not obtained at the time of CMR but early the same morning. The lack of T2 mapping results may be a limitation of this work.

CONCLUSIONS

Our findings favor the use of CMR T1 mapping and echocardiographic GLS in HTx patients to guide more selective EMBs, diminish biopsy-related complications, and fine-tune immunosuppressive treatment. Whether CMR T1 mapping and speckle-tracking strain are helpful in determining ACR in biopsy-negative cases with high suspicion needs further investigation.

ADDRESS FOR CORRESPONDENCE: Dr. Leyla Elif Sade, Department of Cardiology, Baskent University, Başkent Üniversitesi Kardiyoloji Anabilim Dalı, 10. Sokak No:45 Bahcelievler, 06490 Ankara, Turkey. E-mail: sadele@gmail.com.

PERSPECTIVES

COMPETENCY IN PATIENT CARE AND PROCEDURAL SKILLS:

Native T1 times and ECV reflect extracellular expansion including fibrosis, edema, and inflammation that are typical features of ACR, and speckle-tracking strain is a sensitive measure of left ventricular systolic function. Thus, tissue characterization by T1 mapping and functional assessment by strain of the entire myocardium are reliable to confidently rule out grade ≥2R ACR and are complementary to each other to define grade 1R with reasonable accuracy in HTx patients.

TRANSLATIONAL OUTLOOK:

Additional studies are needed to validate noninvasive monitoring of allograft rejection by CMR T1 mapping and speckle-tracking strain against routine biopsies in terms of long-term allograft survival and to test whether noninvasive imaging strategy could risk-stratify patients accurately and defer unnecessary biopsies confidently.

REFERENCES

1. Costanzo MR, Dipchand A, Starling R, et al. The International Society of Heart and Lung Transplantation Guidelines for the care of heart transplant recipients. Revision of the 1990 working formulation for the standardization of nomenclature in the diagnosis of heart rejection. J Heart Lung Transplant 2005;24:1710–20.

2. Everly MJ. Cardiac transplantation in the United States: an analysis of the UNOS registry. Clin Transpl 2008:35–43.

3. Butler CR, Savu A, Bakal JA, et al. Correlation of cardiovascular magnetic resonance imaging findings and endomyocardial biopsy results in patients undergoing screening for heart transplant rejection. J Heart Lung Transplant 2015;34:643–50.

4. Markl M, Rustogi R, Galizia M, et al. Myocardial T2-mapping and velocity mapping: changes in regional left ventricular structure and function after heart transplantation. Magn Reson Med 2013;70:517–26.

5. Badano LP, Miglioranza MH, Edvardsen T, et al. European Association of Cardiovascular Imaging/Cardiovascular Imaging Department of the Brazilian Society of Cardiology recommendations for the use of cardiac imaging to assess and follow patients after heart transplantation. Eur Heart J Cardiovasc Imaging 2015;16:919–48.

6. Stewart S, Winters GL, Fishbein MC, et al. Revision of the 1990 working formulation for the standardization of nomenclature in the diagnosis of heart rejection. J Heart Lung Transplant 2005;24:1710–20.

7. Sade LE, Eroğlu S, Yüce D, et al. Follow-up of heart transplant recipients with serial echocardiographic coronary flow reserve and dobutamine stress echocardiography to detect cardiac allograft vasculopathy. J Am Soc Echocardiogr 2014;27:531–9.

8. White SK, Sado DM, Fontana M, et al. T1 mapping for myocardial extracellular volume measurement by CMR: bolus only versus primed infusion technique. J Am Coll Cardiol Img 2013;6:955–62.

9. Kobashigawa JA, Kirklin JK, Naftel DC, et al., for the Transplant Cardiologists Research Database Group. Pretransplantation risk factors for acute rejection after heart transplantation: a multiinstitutional study. J Heart Lung Transplant 1993;12:355–66.

10. Marie PY, Angioï M, Carteaux JP, et al. Detection and prediction of acute heart transplant rejection with the myocardial T2 determination provided by a black-blood magnetic resonance imaging sequence. J Am Coll Cardiol 2001;37:825–31.

11. Taylor AJ, Vaddadi G, Pfluger H, et al. Diagnostic performance of multisequential cardiac magnetic resonance imaging in acute cardiac allograft rejection. Eur J Heart Fail 2010;12:45–51.

12. Giri S, Chung YC, Merchant A, et al. T2 quantification for improved detection of myocardial edema. J Cardiovasc Magn Reson 2009;11:56.

13. Usman AA, Taimen K, Wasielewski M, et al. Cardiac magnetic resonance T2 mapping in the monitoring and follow-up of acute cardiac transplant rejection: a pilot study. Circ Cardiovasc Imaging 2012;5:782–90.

14. Steen H, Merten C, Refle S, et al. Prevalence of different gadolinium enhancement patterns in patients after heart transplantation. J Am Coll Cardiol 2008;52:1160–7.

15. Miller CA, Naish JH, Shaw SM, et al. Multiparametric cardiovascular magnetic resonance surveillance of acute cardiac allograft rejection and characterisation of transplantation-associated myocardial injury: a pilot study. J Cardiovasc Magn Reson 2014;16:52.

16. Aherne T, Tscholakoff D, Finkbeiner W, et al. Magnetic resonance imaging of cardiac transplants: the evaluation of rejection of cardiac allografts with and without immunosuppression. Circulation 1986;74:145–56.

17. Wisenberg G, Pflugfelder PW, Kostuk WJ, McKenzie FN, Prato FS. Diagnostic applicability of magnetic resonance imaging in assessing human cardiac allograft rejection. Am J Cardiol 1987;60:130–6.

18. Ide S, Riesenkampff E, Chiasson DA, et al. Histological validation of cardiovascular magnetic resonance T1 mapping markers of myocardial fibrosis in paediatric heart transplant recipients. J Cardiovasc Magn Reson 2017;19:10.

19. Clemmensen TS, Løgstrup BB, Eiskjær H, Poulsen SH. Serial changes in longitudinal graft function and implications of acute cellular graft rejections during the first year after heart transplantation. Eur Heart J Cardiovasc Imaging 2016;17:184–93.

20. Sarvari SI, Gjesdal O, Gude E, et al. Early postoperative left ventricular function by echocardiographic strain is a predictor of 1-year mortality in heart transplant recipients. J Am Soc Echocardiogr 2012;25:1007–14.

21. Tang Z, Kobashigawa J, Rafiei M, Stern LK, Hamilton M. The natural history of biopsy-negative rejection after heart transplantation. J Transplant 2013;2013:236720.

22. Ambardekar AV, Alluri N, Patel AC, Lindenfeld J, Dorosz JL. Myocardial strain and strain rate from speckle-tracking echocardiography are unable to differentiate asymptomatic biopsy-proven cellular rejection in the first year

after cardiac transplantation. J Am Soc Echocardiogr 2015;28:478–85.

23. Sera F, Kato TS, Farr M, et al. Left ventricular longitudinal strain by speckle-tracking echocardiography is associated with treatment-requiring cardiac allograft rejection. J Card Fail 2014;20:359–64.

24. Mingo-Santos S, Moñivas-Palomero V, Garcia-Lunar I, et al. Usefulness of two-dimensional strain parameters to diagnose acute rejection after heart transplantation. J Am Soc Echocardiogr 2015;28:1149–56.

25. Eleid MF, Caracciolo G, Cho EJ, et al. Natural history of left ventricular mechanics in transplanted hearts: relationships with clinical variables and genetic expression profiles of allograft rejection. J Am Coll Cardiol Img 2010;3:989–1000.

26. Saleh HK, Villarraga HR, Kane GC, et al. Normal left ventricular mechanical function and synchrony values by speckle-tracking echocardiography in the transplanted heart with normal ejection fraction. J Heart Lung Transplant 2011;30:652–8.

27. Nozyński J, Zakliczyński M, Zembala-Nozyńska E, et al. Remodeling of human transplanted myocardium in ten-year follow-up: a clinical pathology study. Transplant Proc 2007;39:2833–40.

28. Clemmensen TS, Løgstrup BB, Eiskjaer H, Høyer S, Poulsen SH. The long-term influence of repetitive cellular cardiac rejections on left ventricular longitudinal myocardial deformation in heart transplant recipients. Transpl Int 2015;28:475–84.

29. Pichler P, Binder T, Höfer P, et al. Two-dimensional speckle tracking echocardiography in heart transplant patients: three-year follow-up of deformation parameters and ejection fraction derived from transthoracic echocardiography. Eur Heart J Cardiovasc Imaging 2012;13:181–6.

KEY WORDS cardiac magnetic resonance, echocardiography, heart transplant, strain, T1 mapping